Meat Science 152 (2019) 8–19

Contents lists available at ScienceDirect

Meat Science

journal homepage: www.elsevier.com/locate/meatsci

Detectability of the degree of freeze damage in meat depends on analytic-tool selection

Bjørg Egelandsdal[a,*], Sisay Mebre Abie[b], Stefania Bjarnadottir[c], Han Zhu[a], Hilde Kolstad[e], Frøydis Bjerke[c], Ørjan G. Martinsen[b,d], Alex Mason[c], Daniel Münch[f]

[a] Faculty of Chemistry, Biotechnology and Food Science, Norwegian University of Life Sciences, 1432 Aas, Norway
[b] Department of Physics, University of Oslo, 0316 Oslo, Norway
[c] Animalia, Norwegian Meat and Poultry Research Centre, 0513 Oslo, Norway
[d] Department of Clinical and Biomedical Engineering, Oslo University Hospital, 0372 Oslo, Norway
[e] Imaging Centre, Faculty of Biosciences, Norwegian University of Life Sciences, 1432 Aas, Norway
[f] Faculty of Ecology and Natural Resource Management, Norwegian University of Life Sciences, 1432 Aas, Norway

ARTICLE INFO

Keywords:
Meat
Freezing
Cryo-SEM
Nuclear magnetic resonance
Microwave spectroscopy
Bioimpedance

ABSTRACT

Novel freezing solutions are constantly being developed to reduce quality loss in meat production chains. However, there is limited focus on identifying the sensitive analytical tools needed to directly validate product changes that result from potential improvements in freezing technology. To benchmark analytical tools relevant to meat research and production, we froze pork samples using traditional (−25 °C, −35 °C) and cryogenic freezing (−196 °C). Three classes of analyses were tested for their capacity to separate different freeze treatments: thaw loss testing, bioelectrical spectroscopy (nuclear magnetic resonance, microwave, bioimpedance) and low-temperature microscopy (cryo-SEM). A general effect of freeze treatment was detected with all bioelectrical methods. Yet, only cryo-SEM resolved quality differences between all freeze treatments, not only between cryogenic and traditional freezing. The detection sensitivity with cryo-SEM may be explained by testing meat directly in the frozen state without prior defrosting. We discuss advantages, shortcomings and cost factors in using analytical tools for quality monitoring in the meat sector.

1. Introduction

Freezing can extend the shelf-life of meat to > 10 times of that commonly advised for refrigerated storage (Warriss, 2010). Despite this, meat quality deterioration (meat juice loss, flavour and color changes) is often inevitable when products pass through the initial freezing, freeze storage and the final thawing stages (Leygonie, Britz, & Hoffman, 2012; Syamaladevi, Manailoh, Muhunthan, & Sablani, 2012). Thaw loss can also be a major economic factor.

Consumers often perceive frozen foods as less valuable and less attractive alternatives to fresh, unprocessed products (Vanhonacker, Pieniak, & Verbeke, 2013 for fish). Together with the generally lower sales prices, this makes thawed meat attractive for labeling fraud, with as much as 15% and 8% of meat falsely labeled as fresh in Switzerland and the UK respectively (Ballin & Lametsch, 2008). In addition to labeling regulations for thawed vs. fresh meats, the European Council also permits specific labeling of 'quick frozen' foodstuff (EEC, 1989; EEC, 2006), to signal higher quality and market value. Such labeling benefits are particularly relevant for novel freezing solutions that are marketed with improved quality attributes, e.g. by quick freezing (James, Purnell, & James, 2015). Innovations in rapid freezing technology range from already available commercial solutions, such as impingement (Salvadori & Mascheroni, 2002) and cryo-mechanical freezing (Agnelli & Mascheroni, 2002), to mostly pre-commercial, but intensely studied solutions, including pressure assisted freezing (Otero, Rodriguez, Perez-Mateos, & Sanz, 2016; Otero & Sanz, 2012). Ideally, labelling regulations by food authorities and the developments in freezing solutions should be accompanied by adequate research into food quality monitoring.

Traditionally, much analytic effort on frozen meat has been concerned with discriminating fresh from defrosted meat (Ballin & Lametsch, 2008 for review). Among the most relevant methods so far are enzymatic assays, in particular the HADH method (Gottesmann & Hamm, 1987), tests of DNA degradation, e.g., by comet assays (Park et al., 2000), microscopic imaging (Carroll, Cavanough, & Rorer, 1981; Ngapo, Babare, Reynolds, & Mawson, 1999), variants of infrared (IR) or

* Corresponding author.
E-mail address: bjorg.egelandsdal@nmbu.no (B. Egelandsdal).

https://doi.org/10.1016/j.meatsci.2019.02.002
Received 1 July 2018; Received in revised form 30 January 2019; Accepted 4 February 2019
Available online 08 February 2019

visible (VIS) spectroscopy and imaging (Ballin & Lametsch, 2008), hemoglobin-linked color changes (Liu, Barton 2nd, Lyon, Windham, & Lyon, 2004) as well as nuclear magnetic resonance spectroscopy (Mortensen, Andersen, Engelsen, & Bertram, 2006). Among these the electromagnetic methods for fresh - frozen authentication, IR/VIS has been dominating.

Suitable methods for benchmark ('performance') testing the capacity of analytical tools in detecting improvements in freezing technology may include those used for the authentication of frozen meats (described above). However, the potential quality differences (e.g., reduced thaw loss) resulting from freezing can be relatively small and, hence, more challenging to detect. This likely explains that studies testing effects on actual food products are scarce (James et al., 2015).

Light microscopy on stained sections has proven useful for decades for detecting freeze damage since cell damages correlate with the size of ice crystals formed (Martino & Zaritzky, 1988). Classical transmission and scanning electron microscopy reflect the same but at higher resolution. The more recent technique of cryo-electron microscopy allows studying ice crystal cavities and protein or whole tissue assemblies directly in the frozen state. This effectively eliminates possible structural disturbance by subsequent thawing (McDowall, Hofmann, Lepault, Adrian, & Dubochet, 1984). Briefly, frozen meat samples are rapidly transferred into liquid nitrogen, which 'arrests' the frozen state ('cryo-fixation'). Raising the temperature above −100 °C removes all ice ('sublimation') formed by initial freezing, and hence exposes cavities that resemble the original ice crystal formations. Scanning electron microscopy (SEM) then allows imaging these texture irregularities directly and with great depth of field. Limited accessibility of cryo-SEM equipment has probably contributed to the fact that only a few studies have been published on food quality monitoring using the technique. While differences between fresh and freezing treatments can be robustly detected with cryo-SEM, only one study has reported trends towards detecting differences in cavity size caused by different freezing rates (Ngapo et al., 1999).

Low-field nuclear magnetic resonance (NMR) proton T_2 relaxometry is an established, non-invasive spectroscopic method that has been widely used to study physical properties of water in biological material. The method determines the relaxation rate of hydrogen atoms. The relaxation typically occurs with a multi-exponential decay. For muscle tissue, the decay pattern of the NMR relaxation correlates with the distribution of intra- and extracellular water. In particular, intracellular and intrafibrillar water is expected to decline when ice crystal size increases. Three relaxation populations are established from NMR studies in meat: T_{20} (0-10 ms) is linked to bound water, T_{21} (35-50 ms) to fluids trapped within myofibrils and T_{22} (100-250 ms) is linked to free fluids (Bertram & Andersen, 2004; Bertram, Purslow, & Andersen, 2002). What's more, these values are shown to be consistent with structural damage caused by freezing meat at −20 °C and −80 °C (Mortensen et al., 2006).

Bioelectrical impedance (BI) is a well-established tool for medical applications and is also used for food quality monitoring (Pliquett, 2010; Zhao et al., 2017). Impedance measures describe the electrical and dielectric properties of muscle tissue, which essentially comprises resistor-like elements (intra- and extracellular fluids) and capacitor-like elements (cell membranes). This can cause frequency dependent response patterns, where low and high frequency stimulation cause different frequency dispersion. The low frequency 'α-dispersion' (1 Hz–10 kHz) and high frequency 'β-dispersion' (10 kHz–10 MHz) bands are dominated by more resistor- and more capacitor-like contributions, respectively (Damez, Clerjon, Abouelkaram, & Lepetit, 2007; Martinsen, Grimnes, & Mirtaheri, 2000; Pliquett, Altmann, Pliquett, & Schoberlein, 2003; Zhao et al., 2017). Resistor- and capacitor-like elements can make BI sensitive to solute ('water') abundance, fat content, tissue structure and cell damage (Ward, Hopkins, Dunshea, & Ponnampalam, 2016). Since all cell membranes degrade from early post mortem, through chill storage and especially through freezing, intra- and extracellular ions mix to various extents affecting both the capacitance and the resistance pending extent of freeze damage. Yet, how freezing and thawing affect bioelectrical impedance profiles is not much explored. A recent report, however, demonstrated that BI allows distinguishing defrosted from fresh chicken filets (Chen et al., 2017).

Microwave spectroscopy extends bioimpedance measurements into the GHz range by including high frequency bands of the 'γ dispersion' (Damez et al., 2007). Energy absorption in the microwave range is associated with dielectric losses. Among others, water state, ion composition and the actual structure of proteins affect dielectricity. Proteins may change their structure/ dielectric properties when they denature and aggregate, a phenomena that takes place with freezing (Pitera, Falta, & van Gunsteren, 2001). The geometric properties of microwave structures mean that they act as a kind of band-pass filter, allowing some microwave frequencies to pass while suppressing others. This makes identification of molecular phenomena associated with microwaves more challenging (Townes & Schawlow, 2012). Microwave based analysis has recently been applied as a promising technique in the food industry for determining the water holding capacity of raw meat (Mason et al., 2016), and the water activity in a dry-cured ham model (Bjarnadottir, Lunde, Alvseike, Mason, & Al-Shamma'a, 2015). Mason et al. (2016) point to frequencies of relevance for water binding like 4.23 GHz. However, the method's ability for monitoring products subjected to frozen storage has not previously been reported. Microwave sensors utilize non-ionizing radiation and therefore present little risk of harm to personnel or products, while enabling non-contact and non-destructive measurement. Furthermore, the sensors are adaptable to a range of applications and are relatively inexpensive to implement.

In addition to the above methods, that all are sensitive to water in meat, thaw loss are often directly measured using absorption, centrifugation, as well as gravity, for which the EZ-drip loss system is a common example (Otto, Roehe, Looft, Thoelking, & Kalm, 2004). Thaw loss is also a direct meat quality variable affecting the visual appearance of meat in addition to its presumed ability to differentiate between freezing treatments.

Typically, most studies are not directly aimed at identifying the most suitable assays for identification of degree of freeze damage. We have therefore subjected pork loin samples to freezing treatments that model cryogenic freezing, as well as freezing used in common household and industrial settings. Two different slow freezing principles were used, namely freezing at −35 and −25 °C to simulate a small freezing difference. It is known that freezer temperatures between −20 °C and −40 °C affect weight loss differences of loins (Petrovic, Grujic, & Petrovic, 1993).

We aimed at directly comparing the selected methods regarding their detection capacity for between-freeze-treatment differences. A-priori ultralow temperature microscopic imaging (cryo-SEM) was foreseen as a high sensitivity method regarding freeze damage, but with low-field NMR, bioimpedance analysis and particular in microwave based spectroscopy with an option to be equally sensitive. Common thaw loss testing was included as a simple and relevant meat quality assay for differentiating between freezing treatment.

2. Materials and methods

2.1. Pork samples

Pork loin (*Sus scrofa domesticus*, *longissimus thoracis*) samples were collected from Norsvin's Landrace and Duroc animals which were raised at a boar testing station, fed ad libitum, fattened to approximately 130 kg and slaughtered at Nortura Rudshøgda. Slaughtering procedures in agreement with EC guidelines were used.

Pork carcasses were chilled in a succession of three cooling treatments (1 h shock chilling: with −22 °C, air velocity, av. = 2–10 m/s, relative humidity, rh = 80–90%; 3.5 h in −1–2 °C, av. = 0.1–0.2 m/s, rh = 80%, until cutting at 3 °C, av. = 0.1–0.3 m/s, rh = 75%). Testing

began approximately 90 h after slaughtering.

To limit confounding effects of sample heterogeneity (effect of animal) on quality measures, we included an initial sample selection. Three out of six animals were chosen based on similarity using drip loss, pH (WTW 330i pH meter, Germany) and color. Color assessment was performed using the standard CIELAB system with separate testing of lightness (L*) and two chromaticity coordinates (a* = red-greenness, b* = yellow-blueness), measured with a Chroma Meter CR-400 (Konica Minolta Sensing Inc., Japan). The instrument was calibrated using a white ceramic plate (L* = 95.0, a* = 4.57, b* = −2.13). Meat samples were left for blooming for 30 min before measuring at a meat surface temperature of 14 °C. For smaller ø20x20mm samples three spots on each slice were measured at three time points. Drip loss testing (three measurements/slice) was performed with the EZ-drip loss system (Otto et al., 2004; Rasmussen & Andersson, 1996) following the instruction manual by the Danish Meat Research Institute (available at https://www.dti.dk/). For the larger 50 x 50 x 50 mm^3 samples, drip loss was assessed by weight testing before treatment and after leaving them to drip for 24 h post-treatment at 4 °C. The larger samples were removed for thaw loss measurements. To further control within-loin and bilateral heterogeneity, we used a standard sampling and replicate scheme for all three freezing treatments and all analysis tools (Fig. 1). A total of six muscles were tested, collected from both sides of three different animals. For all analysis tools, each freezing treatment was represented by six individual samples: three from the left and three from the right in three different animals (18 samples in total). For microscopy and bioimpedance measurements, meat samples of approximately 50 x 50 x 50 mm^3 were collected with a sharp knife using cutting templates. Circular knifes were used for collecting cylindrical samples with dimensions of ø16 x 20 mm and ø20 x 20 mm for NMR and microwave spectroscopy, respectively. Additional samples were collected solely for temperature monitoring measurements.

2.2. Freezing methods

Loin sample replicates were allocated to three treatments that represented commercial and household freezing solutions with different freezing efficiency. Cryogenic freezing (group '*CRYO-196C*') was carried out in a Styrofoam box filled with liquid N_2 and covered with a lid. Cracking is a typical issue when snap freezing biological material directly in liquid N_2. To avoid such damage, samples were kept above the N_2 surface by placing them on a partly submerged aluminum block. Traditional freezing at −35 °C (group '*TR-35C*') was done using a commercial Frigor freezer (TM 600 Frigor, Denmark); for freezing at −25 °C (group '*TR-25C*') a regular household freezer was used (Evalet, type F30 U). As no airblast/fan technology was used here. All samples were frozen individually, wrapped tightly in cling film and then in aluminum foil. Regarding freezing curves, the parameter Tc defined as the necessary time to lower the core temperature from −1.1 to −7 °C (Bevilacqua, Zaritzky, & Calvelo, 1979) was 234 ± 3 min for freezing at −25 °C and 156 ± 4 (mean and standard error) min for freezing at −35 °C for sample size 50 mm × 50 mm × 50 mm. Tc was about 3.5 times lower for the smaller samples basically in agreement with Planks equation for phase transition time (Plank, 1941).

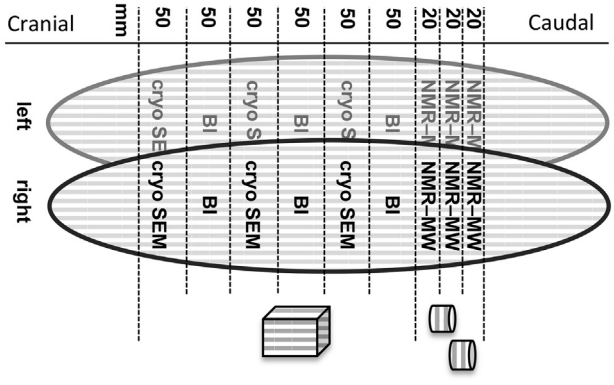

Fig. 1. Sample replicate collection.
To account for within-tissue heterogeneities, samples were collected at different locations for each method. Schematic representation of the collection standard used for the two loins of each animal. Alternating sections from different muscle locations were designated to alternating treatment and analyses groups. Cube-shaped samples were collected for SEM (cryo-scanning electron microscopy) and BI (biompedance). Cylindrical samples were collected for MW (microwave) and NMR (low field nuclear magnetic resonance) spectroscopy and EZ drip-loss.

To ensure complete freezing, and final temperature equilibrium between samples and freezing chambers, all samples were kept in the respective freezers for 3 days. For both non-cryogenic solutions temperature logger information was collected to confirm final temperature values for surface and core of the differently sized samples. To this end, we placed the probes of temperature loggers on the surface and in the center of randomly assigned samples from the six loins prior to freezing (Ebro, EBI 40 and EBI-2 T-313; EU Imtex Business Centre s.r.o., Praha, Czech Republic, compare also Section 3.6).

2.3. Preparations for post-treatment measurements and thaw loss testing

Only cryo-SEM permits measurements directly in the frozen state. Therefore, samples for all other analyses had to be defrosted prior to measurement. Thawing took 60 min from −25 °C to −7 °C core temperature, then 150 min from – 7 °C to −1.1 °C for large samples. The temperature of the samples was stabilized in a chiller at 3 °C.

Small samples for NMR and MW analyses were tested approximately 5 h after thawing was initiated. The larger samples for MW analysis were measured 22 h after thawing started.

Thaw loss was assessed at two time points on the same sample after thawing had begun to represent early 'thaw loss' and later 'post thawing drip loss' (Fig. 2). For all data, weight pre-freezing was used as reference to calculate drip loss percentage. For cryo-SEM, loin samples were kept in a container filled with liquid N_2 until further use.

2.4. Low field NMR

Low field NMR measurements of the transverse spin-spin relaxation time (T_2) were carried out with a Maran Ultra NMR instrument (Resonance Instruments, Witney, UK). The instruments operates at a magnetic field strength of 0.54 T, which corresponds to a proton resonance frequency of 23 MHz. NMR signals were recorded as a sample's response to a traditional Carr-Purcel-Meiboom-Gill (CPMG) pulse sequence (Meiboom & Gill, 1958) with τ = 150 μs, 12 K echoes and 16 transients. The CPMG response curves were fitted to a Maan Ultra integral transform algorithm (R1 Win-DPX software, release 1.2.3, Resonance Instruments, Witney, UK) to obtain a continuous $logT_2$ relaxation time distribution (dI/dlogT2, I = signal intensity of the NMR relaxation curve). The derived relaxation rate distributions were used to obtain T_{22} values and related intensities as described by (Hansen & Zhu, 2016).

Prior to measurements, the cylindrical samples were pierced using a sharp cork borer. Then samples were gently inserted in Teflon holders (diameter 16, length 22 mm), and placed within the homogeneous field section of the radio frequency coil. As before, samples were measured before and after freezing at 4 °C. One measurement was made on three different slides.

2.5. Bioimpedance (BI) measurements

Bioimpedance (Z) comprises resistance (R) and reactance (Xc) elements and can be expressed as follows,

$$\boldsymbol{Z} = R + jX \quad (1)$$

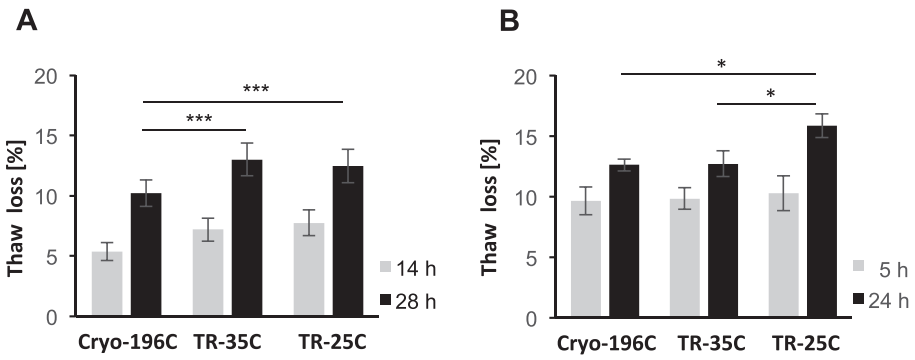

Fig. 2. With thaw loss testing, effects of freezing treatments were not detectable shortly after defrosting started.
A Thaw loss for large samples (50 mm × 50 mm × 50 mm) at 14 h and 28 h after defrosting started. B Thaw loss for smaller samples (ø20x20mm) at 5 h and 24 h. Average values with standard error of means are shown. *** and * indicate Tukey's HSD statistics at $P < .001$ and 0.05, respectively.

$$|\boldsymbol{Z}| = \sqrt{R^2 + X^2} \quad (2)$$

A so called P_y-value (Pliquett et al., 2003) is a well-established parameter to describe bioimpedance and is calculated as follows:

$$P_y = \frac{R_0 - R_\infty}{R_0} \times 100 = \left(1 - \frac{R_\infty}{R_0}\right) \times 100 \quad (3)$$

R_0 and R_∞ are the electrical impedance values at lower and higher frequencies within the same dispersion, respectively, and are obtained using least square curve fitting to the measured data. According to Pliquett et al. (2003) the P_y is between 85 and 95 for fresh meat – depending on meat type – and can decline during storage to $P_y < 10$. Physically, the P_y is a monotonically increasing function of the cell volume fraction surrounded by intact cell membranes.

BI spectroscopy was carried out as transversal measurements (two measurements on two different slices left and right from each animal) using a Sciospec ISX 3 (Sciospec Scientific Instruments GmbH, Germany). The Sciospec ISX 3 has a 4-port interface that was connected to four squarely arranged needle electrodes (spacing 15 mm, diameter = 2 mm). The stimulation frequency was swept from 10 Hz to 1 MHz, providing 30 reading points. The applied voltage amplitude was set to 600 mV peak amplitude. Data was processed with a software package by Sciospec. All before and after freezing measurements were performed in a cold room at 3 °C.

2.6. Microwave spectroscopy

MW spectra were recorded with a Vector Network Analyzer (Rohde & Schwarz ZVL13, München, Germany) and a fixed rectangular resonant cavity, as described in (Mason et al., 2016). The cavity is adapted specifically to accommodate and fix the EZ drip-loss measurement tubes (Mason et al., 2016) and enables a two port configuration, which permits measuring both the power transmitted through (S_{21}), and the power reflected from (S_{11}) the sample (Hiebel, 2008). The design also minimizes the effect of height variation on cavity response. Here we focused on S_{11} measurements, which were recorded for the interval 4–7.5 GHz at 0 dBm (1 mW) power output and approximately 900 kHz resolution bandwidth.

MW measurements were performed before freezing and post-freezing at 3 °C. Prior to measuring, meat samples were placed into EZ drip-loss tubes. Each sample was measured six times at 1 min intervals for one sampling point.

2.7. Cryo-SEM

2.7.1. Sample preparation and cryo-scanning electron microscopy

In all preparation stages prior to microscopy, particular care was taken to avoid exposing the frozen meat to the higher ambient temperatures of the lab. Samples were kept either directly in liquid N_2 or on an aluminum block cooled by N_2 (compare 2.2). To trim samples for microscopy, meat samples were first fractured along the fiber direction, generating pieces that were approximately 5 mm wide (cross section diameter) and 10 mm long. These were then mounted with Tissue-Tek onto modified sample holders, so that the cross-sectional plane was aligned with the microscopic plane. After mounting to a rod, samples were quickly transferred into a liquid N_2 slush (Gatan ALTO 2100, UK). A final cross-sectional cut – to expose the later scanned surface – was performed with a bone cutter (Fine Science Tools, Germany), again in liquid N_2 to minimize condensation and ice buildup on the surface. Finally, the sample was transferred to the N_2 cooled preparation chamber attached to the microscope, then depressurized and moved into the scanning chamber.

Scanning electron microscopy (SEM) images were taken with a Zeiss EVO50 EP, equipped with a cryo-preparation system (Gatan ALTO 2100, UK). To remove ice-crystal buildup and expose cavities formed by ice crystal damage, we initially determined the temperature and time needed for practically complete ice sublimation. This was achieved by raising the temperature in the microscopy chamber from −150 °C to −60 °C within 12 min. For assessing cavity formation we scanned the cross-sectional plane for 6 samples per treatment. Each individual sample was represented by at least three different images taken at 200× magnification (> 60 images in total). For imaging anatomic features at a higher magnification (500×), sample surfaces were additionally coated with gold for 120 s using a sputter coater (Polaron SC7640, Quorum Technologies, UK). All samples were scanned with a low acceleration voltage (EHT) of 1.2 kV for uncoated and with 5.0 kV for gold-coated surfaces (probe current 50pA).

2.7.2. Image analysis

Micrographs were first studied for potential freezing artifacts, i.e. cavities formed by ice crystals, by visual inspection only. While large differences can be robustly identified this qualitative approach, the identification of smaller differences typically calls for quantitative analyses. To this end, automated or manual quantification of microscopic images requires an initial, unbiased image segmentation process. Segmentation generates binary images, where objects of interest, e.g., circular structures, are seperated from the background (e.g., Wolschin, Münch, & Amdam, 2009). However, an unbiased and robust identification of cavity-like objects in cryo-SEM images of frozen meat is complicated by (i) the relatively low signal-to-noise ratio for cavity-like objects due to the large depth of field scanning-electron micrographs, by (ii) highly irregular damage (cavity-like) patterns, and by (iii) extensive tissue deterioration, which impedes the identification of directly comparable structures. More specifically, regions with mostly muscle fibers versus areas with connective tissue could not be reliably identified in damaged meat. To obtain a measure, which represents an overall evaluation of the complex images and to minimize the risk of biased object detection or a biased selection of a non-representative sub-selection of quantified objects, we have chosen a semi-quantitative approach based on observer rankings. In brief, 14 observers naive to treatment identity were asked to rank a set with SEM images, where all individual samples were represented by three replicate images (all at

200× magnification). Observers were asked to rank the micrographs using a scale between 1 and 5, with 1, representing "small or undetectable cavities" to 5, representing "very large cavities". Prior to ranking, the observers were trained with a ranking key. The key provided two images per rank, and was generated to train observers to the full range of cavity sizes found in the entire image set. To choose representative images for the key, all 200× images were sorted from low to large cavity size by a person naive to treatment groups. According to the sequence of sorting, images were selected to represent the respective ranks between 1 and 5.

2.8. Statistical analysis

The data processing and statistical analyses were done with Excel (Microsoft Inc.), Minitab (v.17, Minitab Inc., USA), Statistica (v.11.0, Statsoft/Dell Inc.), 50–50 MANOVA Windows version (Prediktor, 2016) and Unscrambler X (v.10.5, Camo Software AS, Oslo, Norway).

Generally, all spectral data were subjected to similar calculations in a defined sequence. In contrast to cryo-SEM, a pre-freezing (fresh) control was included for all bioelectrical analyses as a reference. Hence, the data matrix for bioelectrical analysis consisted of the design variables treatment (N = 3) and animal origin (N = 3), as well as fresh/defrosted relations. These three sub-matrices were combined and subjected to the analyses detailed below.

First, 50–50 MANOVA was used to explore possible effects in the multivariate spectral data ('raw data'). This method is highly effective for calculation effects for designed data with many strongly correlated responses such as spectra (Langsrud, 2002). Second, cross-validated (random validation) Partial Least Square (PLS) regression models were used to generate prediction plots with predicted freezing temperatures for each treatment group. PLS does not calculate effects of the design variables as such, but is particularly useful when there is multi-collinearity among X variables, such as the wavelengths of a spectrum. The direct comparison of predicted temperature values and actual freezing temperatures is an informative indicator of the measurement accuracy of each method. PLS regression was carried out by testing a panel of pre-processing techniques, including standardization of data based on standard deviation, first derivative, second derivative normalization, and for selected tests also weighting according to individual thaw loss (for the impact of preprocessing on multivariate analyses compare Martens & Geladi, 2004; Rinnan, van den Berg, & Engelsen, 2009). For MW analysis, pre-processing in addition included subtraction of mean spectra according to Mason et al. (2016). Mean centering of spectra was used for multivariate analysis.

Third, we explored the use of established derived parameters for freeze treatment identification, including P_y for BI (Pliquett et al., 2003) and T_2 for NMR (Bertram et al., 2002). As the relevance of individual frequencies or frequency bands is not yet established for MW analyses of freeze treated meat, variable selection was performed using PLS analysis. More specifically, we selected frequencies based on regression coefficients obtained by PLS analysis (significant at $P < .05$) in order to identify frequencies that maintained maximum prediction accuracy. Finally, P_y and T_{22} along with selected MW frequencies were subjected to ANOVA models (main factors treatment and animals plus interactions) and Tukey post-hoc testing.

ANOVA models were calculated for both, temperatures predicted by PLS models using complete data set (see before) and for the extracted parameters (previous section). This allowed comparing how freezing treatments were distinguished by analyses that are either based on 'raw spectra' or on extracted variables.

Ranking data for cryo-SEM images was analyzed with a non-parametric Kruskal–Wallis one-way analysis of variance and post-hoc Mann-Whitney U testing.

3. Results and discussion

3.1. Grading raw material quality attributes to evaluate between-sample heterogeneity

Since the study focused on the sensitivity of analytical tools for effects of freeze treatments, we included a pre-selection process to compress potential effects of animal origin. Pre-selection of animals was based on the quality attributes pH, drip loss and color, but did not entirely eliminate effects of animal origin (see Table S1 for results and statistics). We therefore included animal origin as a factor in all models.

3.2. Individual assessment of a tool's detection capacity for freeze-related quality deterioration

The following sections evaluate five analytical tools separately. We expected that highly sensitive tools can differentiate between all individual freeze treatments, i.e. also between the two traditional freezing solutions with more similar freezing rates (group '*TR-35C*' vs. group '*TR-25C*'). In contrast, we expected less sensitive tools to only differentiate between rapid cryogenic freezing (group '*CRYO-196C*') on the one hand and traditional freezing on the other hand ('*TR-35C*' and '*TR-25C*'). The least sensitive methods were expected to only differentiate between fresh and defrosted meat.

3.2.1. Thaw loss

Two different sample sizes were tested with larger samples representing sample dimensions tested with bioimpedance and cryo-SEM, and smaller samples representing sample dimensions tested with low-field NMR and microwave spectroscopy. For both large and small samples, we did not detect an effect of freeze treatment early after defrosting (Fig. 2A for 'thaw loss' in large samples after 14 h: Fig. 2B for 'thaw loss' in small samples after 5 h; ANOVA treatment effect for large samples: $df_{large,14h} = 2$, $F_{large,14h} = 3.39$, $P_{large,14h} = 0.084$, for small samples: $df_{small,5h} = 2$, $F_{small,5h} = 0.28$, $P_{small,5h} = 0.764$). However, an animal replicate effect was detected for large samples at this early time point (ANOVA, $df_{large,14h} = 2$, $F_{large,14h} = 16.87$, $P_{large,14h} < 0.001$). In contrast, a significant effect of freeze treatment became detectable within a second time window to assess 'post-thawing drip loss' (Fig. 2A for drip loss in large samples after 28 h; Fig. 2B for drip loss in small samples after 24 h; ANOVA treatment effect for large samples: $df_{large,28h} = 2$, $F_{large,28h} = 9.03$, $P_{large,28h} = 0.014$; ANOVA treatment effect for small samples: $df_{small,24h} = 2$, $F_{small,24h} = 3.88$, $P_{small,24h} = 0.048$). Also, 24 h and 28 h after thawing had begun, thaw loss testing did not detect differences between all individual freeze treatments – neither for the larger or the smaller samples (Fig. 2A and B for Tukey's post hoc statistics). In addition, between-treatment effects were not consistent for the two sample sizes: no thaw loss difference was detected between *TR-35C* and *TR-25C* in larger samples, whereas no thaw loss difference was detected between *CRYO-196* and *TR-35C* in smaller samples. An animal effect was again significant for large samples after 28 h (ANOVA: $df_{large,14h} = 2$, $F_{large,14h} = 17.9$, $P_{large,14h} < 0.001$).

In conclusion, thaw loss testing shortly after defrosting was not suitable to separate freeze-related quality differences. Freeze treatment effects became first detectable after > 24 h had passed. Bearing in mind that since the animal effect was minimized here, thaw thaw loss may not globally resolve differences between all the individual freeze treatments. In line with our results, a study with hamburger meat also failed to detect early thaw-loss differences between cryo- and traditional freezing shortly after defrosting, but could detect differences between freeze treatments after 24 h (Agnelli & Mascheroni, 2002).

3.2.2. Biophysical measurements

Effects of freezing on biophysical properties of meat were assessed using low-field NMR (NMR), bioimpedance (BI) and microwave

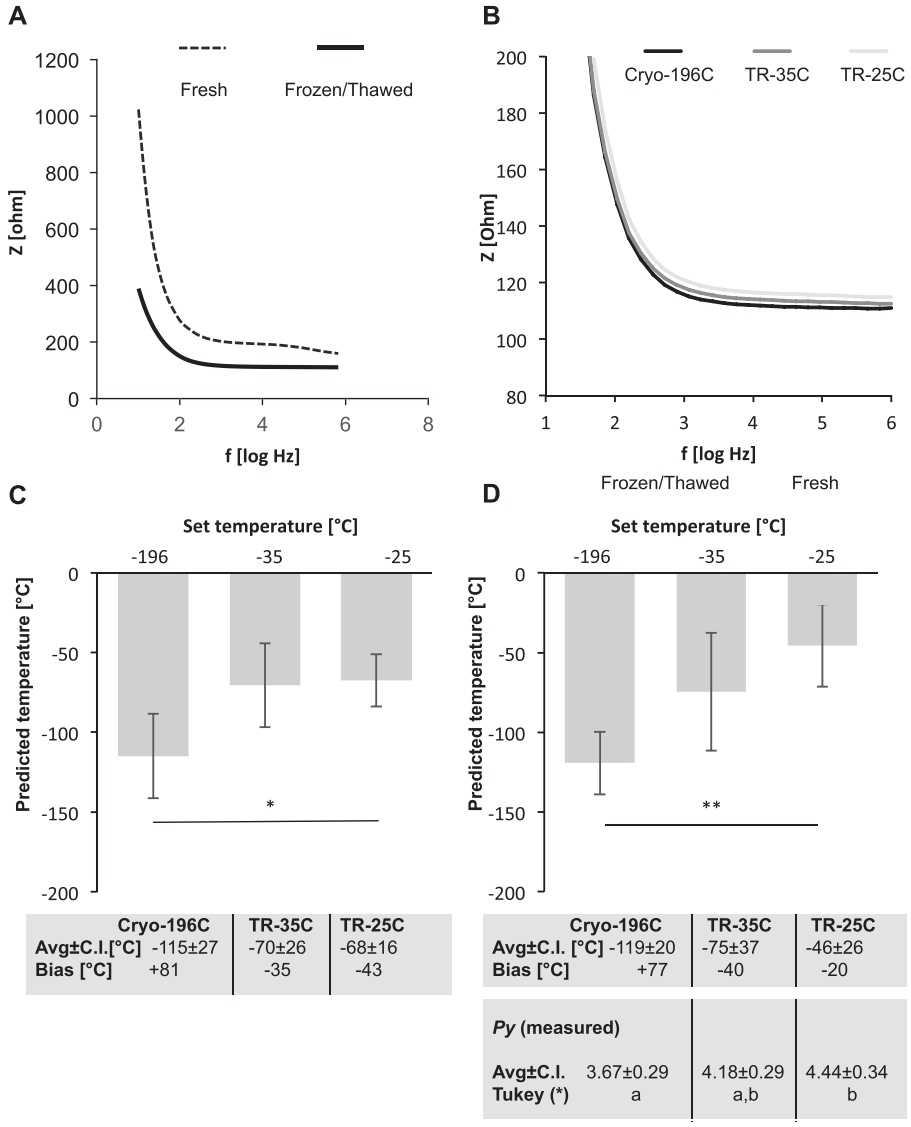

Fig. 3. Detection of freeze treatment effects with bioimpedance (BI) spectroscopy.
A BI spectra (median *Z*-profiles) for fresh and defrosted meat samples. B Mean BI spectra for the three tested freezing treatments (see 2.2 for treatment groups). C Treatment comparisons based on temperatures (means and standard deviations) predicted by the PLS model using the *z*-profiles. D Treatment comparisons based on P_y. ** and * indicate Tukey's HSD statistics at $P < .01$ and 0.05, respectively. The confidence interval (C.I.) with predicted means are indicated together with the model bias.

spectroscopy (MW).

3.2.2.1. Differentiating fresh from defrosted meat with bioelectrical and magnetic measurements. As an initial proof-of-concept validation, we asked if all spectroscopic assays have the capacity to distinguish the relatively large differences that are expected between fresh meat samples ('tested before freezing') and defrosted meat ('tested after freezing'; see Figs. 3A, 4A and 5A). Cryo-SEM is not the standard imaging application for testing thawed samples, and therefore is not tested in this context.

Bioimpedance (BI) spectra of fresh and defrosted samples differed significantly (Fig. 3A; 50–50 MANOVA, df = 1, P < .001, explained variance = 23.0%). No effect for the factor meat origin (i.e. animal) was detected. Entire low-field nuclear magnetic resonance (NMR) spectra included bands for all three relaxation rates, and were significantly different in fresh and defrosted samples (Fig. 4A, 50–50 MANOVA, df = 1, P < .001, explained variance = 64.6%). The rather high *explained variance* indicates that NMR spectra can be good predictors for authenticating fresh vs. defrosted meat. No effect of meat origin was detected (50–50 MANOVA, df = 2, P > .05). Similar to BI and NMR, entire microwave (MW) spectra for reflected power measurements (S_{11}) differed significantly in fresh and defrosted samples (Fig. 5A; 50–50 MANOVA, df = 1, *explained variance* = 16.9, P < .001, standardization by 1/sdev). The effect of animal replicate was now significant (50–50 MANOVA, df = 2, explained variance = 13.2, P < .001, standardization by 1/sdev).

In conclusion, comparing fresh and defrosted meat, an effect of freezing was detected by all three biophysical methods. However, an *explained variance* of 64.6% indicates a superior detection performance for low-field NMR, as compared to BI and MW spectroscopy. NMR relaxation rates separated all fresh from all defrosted samples and compares with various principles of NIR regarding differentiation ability (Barbin, Sun, & Su, 2013; Thyholt & Isaksson, 1997).

3.2.2.2. Differentiating quality attributes between traditional and cryogenic freezing solutions with bioelectrical and -magnetic measurements. We next tested if the spectroscopic methods could also detect potentially smaller quality differences caused by the three different freezing treatments.

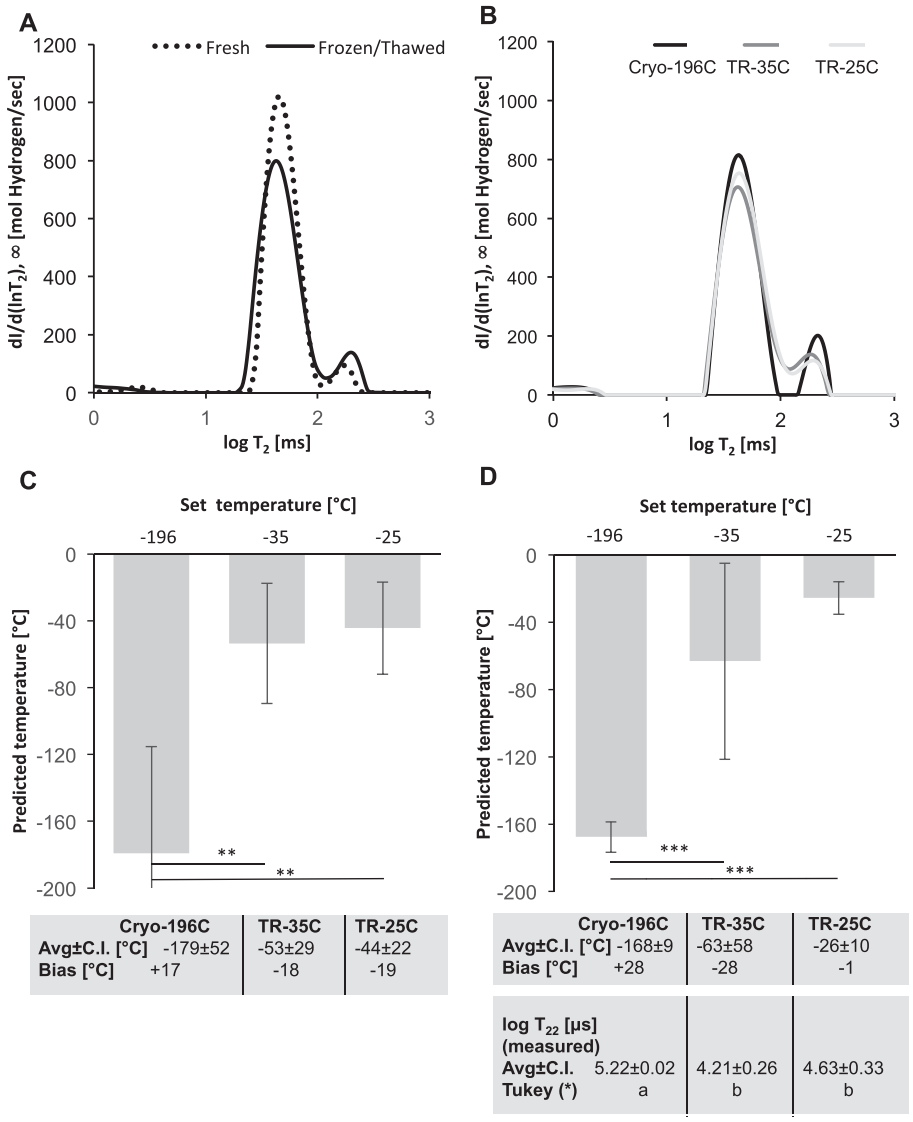

Fig. 4. Detection of freeze treatment effects with low-field relaxation NMR spectroscopy.
A Mean NMR spectra for fresh and defrosted meat samples. B Mean NMR spectra for the tested freezing treatments (compare 2.2). C Treatment comparisons based on temperatures (means and standard deviations) predicted by the PLS model of NMR spectra. D Treatment comparisons based on T22. *** and ** indicate Tukey's HSD statistics at P < .001 and 0.01, respectively. The confidence interval (C.I.) with predicted means are indicated together with the model bias.

Data for all three methods were analyzed consistently by using a sequence of statistical approaches (see Section 2.8 and 3.4).

3.2.2.2.1. Low-field nuclear magnetic resonance (NMR) spectroscopy. By contrasting raw spectral data that includes the temporal bands for all three relaxation rates (1 ms–250 ms; Fig. 4B) we found an overall effect of freeze treatment on NMR response (50–50 MANOVA, df = 2, P = .049, *explained variance* = 26.0%). Yet, the NMR response was also affected by the factor animal origin (50–50 MANOVA df = 2, P = .005, *explained variance* = 35.4%), with *explained variance* being higher for the factor animal replicate than for treatment.

As before, we used a cross validation PLS model to examine how the entire spectral data could predict, or separate, the three individual freezing methods. Fig. 4C shows that predicted temperatures (validated model $R^2 = 0.28$, nPC = 3) ranged from approximately −179C to −44C, with the lowest temperatures being correctly assigned to the *CRYO-196C* group, and higher temperatures to traditional freezing treatments *TR-25C*. The predicted temperatures significantly separated *CRYO-196C* vs. *TR-35C* (Tukey's, *T* = 3.97, P = .008) and *CRYO-196C* vs. *−25C* (Tukey's, *T* = 4.17, P = .006), but not between the two traditional freeze-treatments *TR-35C* and *TR-25C* (*T* = −0.20, P = .978).

We then asked if individual relaxation parameters can predict and separate treatment identity. We only found a significant effect of treatment for T_{22} (ANOVA, df = 2, P < .001 *explained variance* = 77.7%, Fig. 4D), but not a significant effect for animal origin (df = 2, P = .664, *explained variance* = 1.6%). For the relaxation parameters T_{21} treatment was not significant (df = 2, P = .116, *explained variance* = 17.6) but then the animal origin was significant (df = 2, P = .016, *explained variance* = 45.6%). Similar to PLS analysis of the raw spectra, T_{22} based analyses separated very low temperature freezing (*CRYO-196*) from both traditional freeze treatments (Tukey's for *CRYO-196* vs. *TR-35C*: *T* = 5.23, P < .001, Tukey's for *CRYO-196* vs. *TR-25C*: *T* = 7.11, P < .001, Fig. 4D). No difference was detectable between the two traditional freezing methods (Tukey's for *TR-35C* vs *TR-25C*: *T* = 1.88, P = .178). The difference in measurement error explains why *CRYO-196* and *TR*-35C was not separated (Fig. 4D).

Together, NMR analyses based on raw spectral data and on the relaxation parameter T_{22} revealed that NMR spectroscopy is sensitive to freeze treatment. NMR data allowed distinguishing between cryogenic (*CRYO-196C*) and both traditional freezing treatments, but not between *TR-35C* and *TR-25C*. This detection capacity was unaffected by the

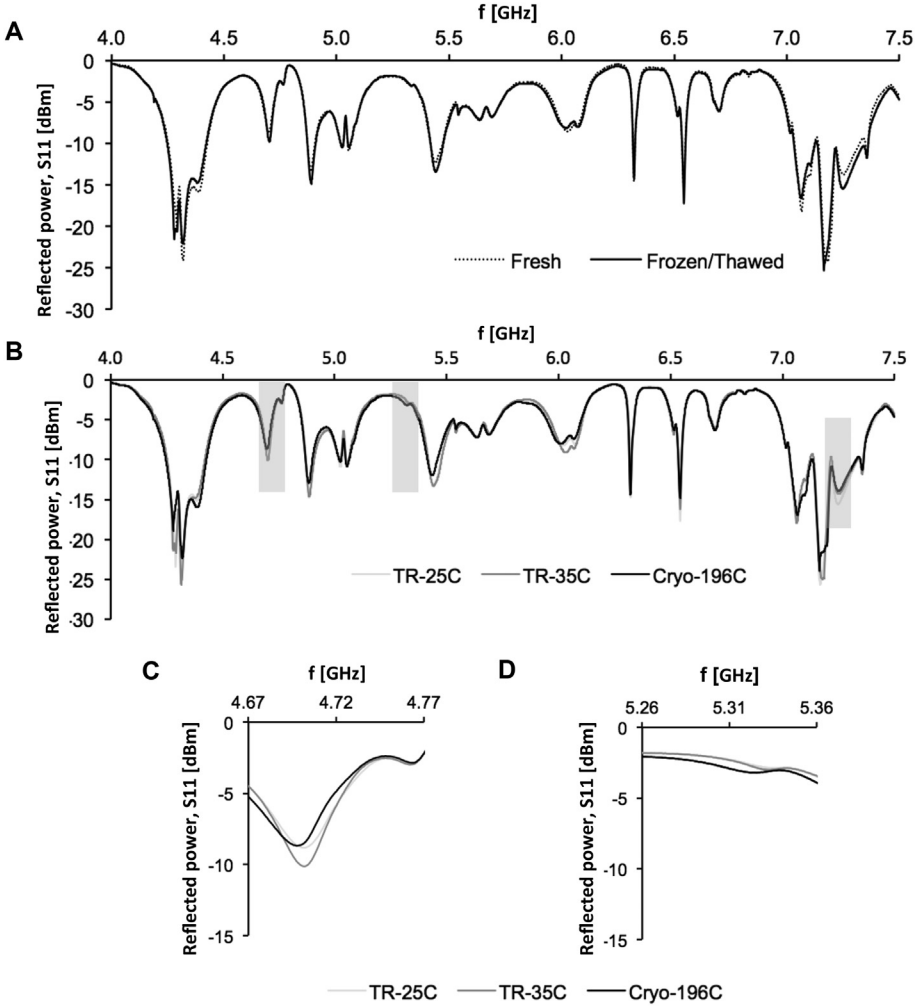

Fig. 5. Detection of freeze treatment effects with microwave (MW) spectroscopy.
A Mean MW spectra for fresh and defrosted meat samples. B Mean MW spectra for the three freezing treatments (compare 2.2). C Frequency bands around frequencies that are predictive of freezing treatment (higher resolution, compare result section 3.2.2.2.3).

particular analysis approach that was chosen.

3.2.2.2.2. Bioimpedance (BI) measurements. We first contrasted raw spectral response data including α- and β-dispersion bands (10 Hz–1 MHz, Fig. 3B), and detected an overall effect of freeze treatment (50–50 MANOVA; df = 2, P = .008, *explained variance* = 9.6%). The low *explained variance* indicated that the entire BI spectrum was not a good predictor of overall freeze treatment effects. No replicate effect for animal origin was detected.

The cross-validated PLS model (R^2 = 0.080, nPC = 3) predicted temperatures for the three freezing treatments that ranged from −68 °C to −115 °C, with the lowest temperatures found for the *CRYO-196C* group, and highest temperatures for *TR-35C* and *TR-25C* (Fig. 3C). However, pairwise comparison of the PLS statistics only revealed significant differences between the lowest and highest freezing temperatures (*CRYO-196C* vs. *TR-25C*, Tukey's, *T* = 2.84, P = .032). *CRYO-196C* vs. *TR-35C* were only separated if the interaction term was removed (Tukey's, *T* = 2.66, P = .044), and *TR-35C* was not separated from *TR-25C* (Tukey's, *T* = 0.18, P = .983).

Secondly, we contrasted the different treatments using P_y, an established, derived impedance measure. Similar to testing raw spectral data, ANOVA analyses of P_y revealed a significant effect of freeze treatment (df = 2, F = 19.7, P = .001). With a *explained variance* of 46.7%. P_y was a better predictor of treatment effects than the raw spectral response data. However, similar to PLS analysis of the spectral data, pairwise comparisons revealed significant quality differences between *CRYO-196* and *TR-25C* (Tukey's, *T* = 3.67, P = .006), but not for *CRYO-196* and *TR-35C* (Tukey's, *T* = 2.23, P = .099) or between *TR-35C* and *TR-25C* (Tukey's, *T* = 1.44, P = .346, Fig. 3D). In contrast to the PLS based analysis on raw spectra, the ANOVA based P_y based analysis revealed a significant effect of animal replicate (df = 2, P = .001, *explained variance* 36.7%). This may suggest that large raw material variation may mask effects of freezing treatment.

In conclusion, overall freeze treatment effects could be detected with BI spectroscopy. Yet, BI only separated quality attributes caused by very rapid cryogenic freezing (*CRYO-196C*) from traditional freezing (*TR-35C* and *TR-25C*).

3.2.2.2.3. Microwave (MW) spectroscopy. We first contrasted the raw MW spectra (Fig. 5B) and found a significant overall effect for freezing treatment (50–50 MANOVA, df = 2, P < .001, standardization through 1/sdev) and also for animal replicate (50–50 MANOVA, df = 2, P < .001, standardization through 1/sdev). Yet, especially for treatment the effect size was relatively low (*variance explained* = 5.3% for treatment, *explained variance* = 19.6% for animal replicate).

The PLS model (R^2 = 0.72 with 4 validated PLS factors) using MW spectra predicted temperatures that ranged between −181 °C for the *CRYO-196C* group and − 34 °C for traditional freezing (*TR-35C*, Fig. 6A). The predicted temperatures were significantly different between *CRYO-196* and one traditional freezing solution (Tukey's for *CRYO-196* vs. *TR-35C: T* = 56.32, P < .001, Tukey's for *CRYO-196C*

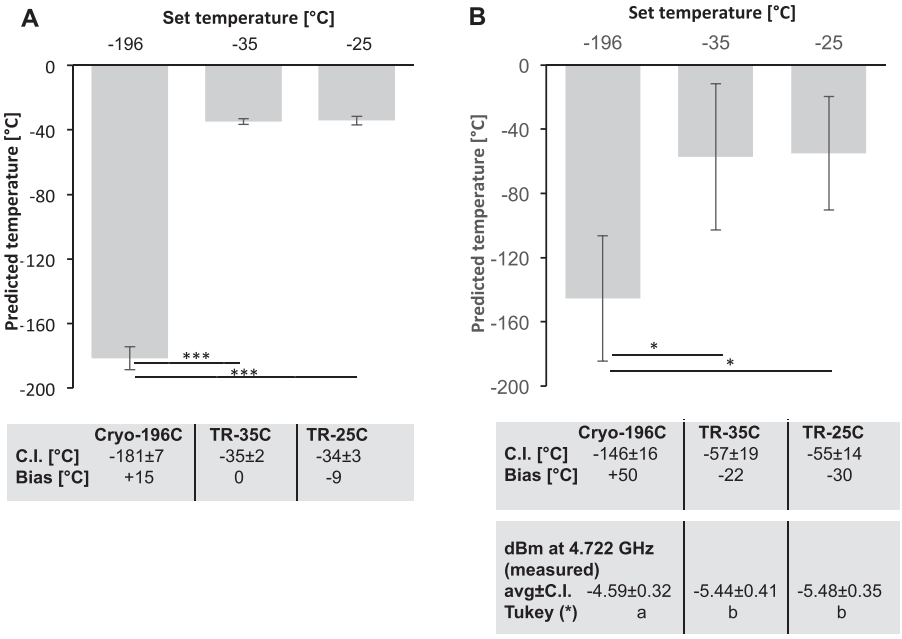

Fig. 6. Detection of freeze treatment effects with microwave (MW) spectroscopy.
A Treatment comparisons based on temperatures (means and standard deviations) predicted by the PLS model of MW spectra (compare Fig. 5). B Treatment comparisons based on a frequency predicted by PLS modeling (4.722GHz). *** and * indicate Tukey's HSD statistics at $P < .001$ and 0.05, respectively. The confidence interval (C.I.) with predicted means are indicated together with the model bias.

vs. *TR-25C*: $T = 56.96$, $P < .001$) but not for *TR-35C* versus *TR-25C* ($T = 0.64$, $P = .801$).

MW spectroscopy is a relatively new quality-monitoring tool in meat science and – to our knowledge – no previous studies have directly aimed at analyzing freezing effects using the technique. We therefore asked if performance in detecting freeze related quality differences could be improved by selecting individual frequency bands, which may be most sensitive to treatment effects. PLS regression with an uncertainty test for each frequency was used for this purpose. Individual frequencies were first identified based on a $P < .05$ cut-off. A cross-validated PLS regression model was then established ($R^2 = 0.85$, 3 validated PLS factors). However, only seventeen regions (7% of the data measured) were selected by the uncertainty test as highly significant ($P < .001$). The following regions of the microwave spectra were then selected [GHz]: 4.09–4.31, 4.43–4.85, 4.88–4.97, 5.04–5.05, 5.13–5.43, 5.46–5.59, 5.65–5.67, 5.83–6.10, 6.30–6.34, 6.50–6.54, 6.70–6.77, 6.83–7.02, 7.05–7.10, 7.14–7.21 7.34–7.36, 7.41–7.42. The ability to predict freezing temperature was unchanged if only these spectral regions were used in calculations. The magnitudes of the P-values suggested the following discrete frequencies as most relevant for treatment detection [GHz]: 4.276, 4.314, 4.453, 4.683, 4.722, 4.830, 4.935, 5.042, 5.181, 5.306, 5.656, 5.965, 6.032, 6.100, 7.166, 7.214 and 7.415. Only 5.65GHz was reported by Mason et al. (2016). It should be pointed out that in principle only three 'frequencies or independent frequency bands' would be needed to predict treatment since 3 PLS factors were used and the 17 frequencies above must be correlated. However, the present may not be a universal result and therefore all 17 frequencies should be tested and verified in future studies. The predicted frequencies were then tested with ANOVA for main effects of freeze treatment and animal replicate (S2 in supplemental materials). Out of the above 17 frequencies, we detected a significant ($P < .05$) treatment effect on amplitude for 3 frequencies and an effect of animal replicate for 2 frequencies (see S2). This may seem disappointing but as more information about treatment is also covered in the interaction term and used in a PLS analysis, most selected frequencies may actually be susceptible to treatment.

Selective frequencies, i.e. frequencies with a high treatment to animal replicate effect ratio, were 4.314GHz (61:1 for treatment relative to animal effect), 4.722GHz (13:1) and 5.306GHz (7.5:1); the first one being closest to Mason et al. (2016). Frequencies mostly sensitive to animal replicate were 7.214GHz and 6.100GHz (Table S2). Fig. 6B shows that the frequency response at 4.722GHz separated ultra-low temperature freezing (*CRYO-196*) from both traditional freeze treatments (Tukey's for *CRYO-196* vs. *TR-35C*: $T = 2.89$, $P = .043$, for *CRYO-196* vs. *TR-25C*: $T = 2.92$, $P = .041$) but did not reveal differences between *TR-35C* and *TR-25C* (Tukey's for *TR-35C* vs. *TR-35C*: $T = 0.03$, $P = .999$). Analysis of the response at 4.722GHz revealed a larger bias than testing the entire spectral response (compare Fig. 6A and B).

Testing of MW responses based on raw spectral data and on a selected frequencies can detect overall effects of freeze treatment and also allowed separating between cryogenic (*CRYO-196C*) and both traditional freezing treatments (*TR-35C, TR-25C)*. The rather large influence of animal origin may have affected the method's ability to detect freezing treatments. In addition, and in contrast to BI and NMR, links between quality attributes (e.g., thaw loss, protein denaturation) and responses for individual frequency bands are not understood. Studying such links will be all the more important, as our data shows that treatment effects between freezing groups are not consistent for the entire frequency range (compare 5C and 5D).

3.2.3. Cryo-SEM

To identify potential differences caused by freeze treatments we took microscopic images of frozen samples without prior thawing (see Section 2.7). Cryo-SEM micrographs were then analyzed for cavities – a most common indicator of ice-crystal formation and freeze damage (Ngapo et al., 1999). Visual inspection of the image set revealed large differences between treatment groups (Fig. 7). Specifically, cavities were readily identifiable and considerably larger in traditionally frozen samples (*TR-35C*, *TR-25C*, arrowheads in Fig. 7) as compared to cryo-frozen meat (*CRYO-196C*). Similarly, tissue integrity, i.e. the regular arrangement of muscle fibers interspersed with perimysial connective tissue (asterisks and arrows in Fig. 7D), is essentially lost, and typical anatomic structures of meat became non-identifiable in *TR-35C* and *TR-25C* (Fig. 7E and F). Most extensive cavity formation was observed with slowest freezing at −25 °C (*TR-25C*, Fig. 7F). Sample-to-sample variation in *TR-25C* and *TR-35C* was noticeable, but it is not possible determine clear differences between these groups with qualitative analysis only. The irregular appearance of damage patterns makes reproducible image segmentation and direct measurements of individual cavities difficult.

Using the semi-quantitative ranking approach described in part 2.5.,

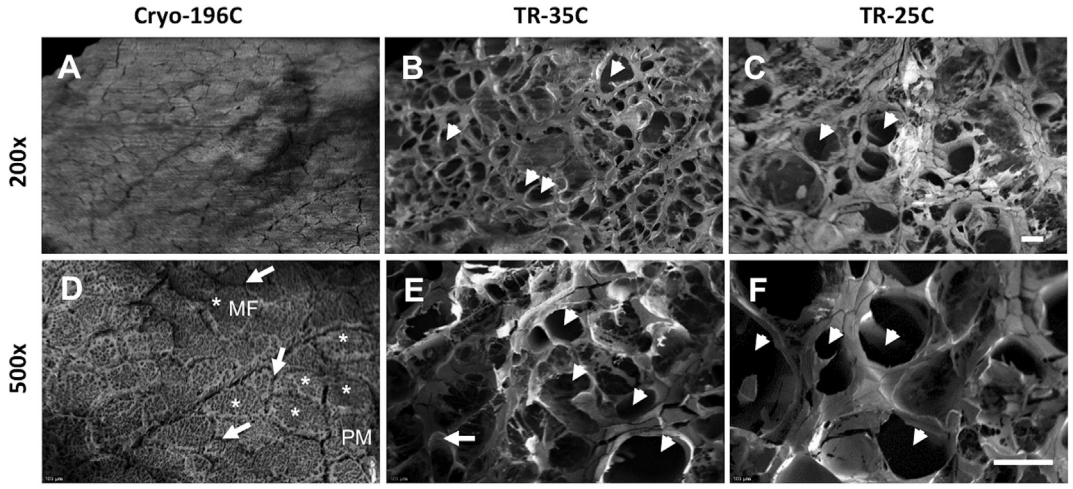

Fig. 7. Cryo-SEM micrographs showing how tissue damage differs among freeze treatments. A-F.
Representative cryo-SEM images for pork loin frozen with liquid N_2 at approximately −196 °C (A, D), and in traditional freezers at −35 °C (B, E) and at −25 °C (C, F). Images A-C and D-F were recorded at 200× and 500× magnification, respectively (scale bar = 100 μm for A-C in C, for D-F in F). Large cavities are indicative of damage by extensive ice-crystal formation, and were evident with traditional freezing at −35 °C and − 25 °C (arrowheads). In addition, characteristic morphological features such as the separation of individual muscle fibers (MF, arrows) by connective tissue (perimysium, PM, asterisks) remained mostly intact only in cryogenically frozen samples (A,D).

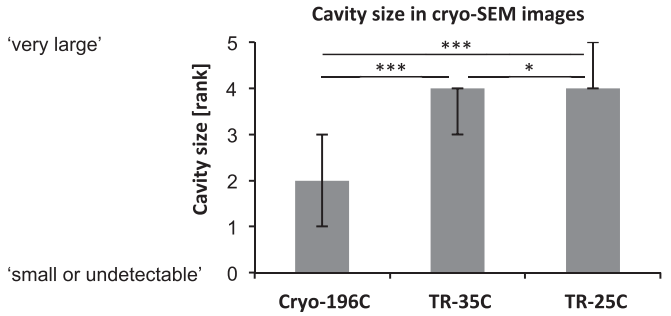

Fig. 8. With semi-quantitative analysis of cryo-SEM images significant differences were detected between all three freeze treatments.
Analyzing a key ice damage attribute (cavity size) through visual evaluation and ranking by 14 observers revealed significant quality differences between all individual freezing treatments (median and quartiles, * and *** depict significance levels of the Mann Whitney U statistics).

we detected an overall effect of freezing temperature on cavity size (Kruskal Wallis, $H_{N=700} = 337.44$, $P < 0{,}001$). Importantly, evaluating data from multiple observers we detected differences in cavity size between all individual freezing treatments (Mann Whitney U/MWU, $Z_{Cryo\text{-}196C \text{ vs } TR35C} = -15.15$, $P \leq .001$; $Z_{Cryo\text{-}196C \text{ vs } TR25C} = -15.74$, $P \leq .001$; $Z_{TR35C \text{ vs. } TR25C} = -2.07$, $P = .039$, Fig. 8). We tested for observer effects, common to sensory analyses, and found a small significant effect (Kruskal Wallis test, $H_{N=700} = 25.31$, $P = .210$). The *explained variance* by the treatment was calculated for all other methods, but is not provided by a non-parametric MWU. However, using a parametric ANOVA on image ranking data we report that 50.1% ($P < .001$) of the variation is explained by freezing treatment, while only 3.3% ($P < .001$) by an effect of observer identity.

In summary, inspection of cryo-SEM images revealed large differences between samples that were frozen cryogenically at −196 °C and those that were traditionally frozen. While the exact freezing conditions of the three treatments we tested here differed from previous studies, our images are in line with the extensive damage patterns and large cavities with diameters > 10 μm that were shown for a slow-freezing protocol (TC [−1 °C, −7 °C] of 60 min, Ngapo et al., 1999). In addition, both visual inspection and our semi-quantitative analyses support small and detectable differences also between the slower, traditionally frozen groups (*TR-35C* vs. *TR-25C*).

3.3. Possible interaction of thaw drip loss and biophysical measurements

When meat samples are frozen and thawed, meat juices will leak from samples in a time dependent manner. Drip loss will therefore add to deterioration patterns that emerge during freezing and freeze storage. In contrast to cryo-SEM, all biophysical measurements used defrosting prior to measurements. Hence, spectral data can be affected, and perhaps may even represent thawing and post-thawing drip loss. Such linkage is known for low-field NMR, which is sensitive to changed liquid distribution among different muscle tissue compartments, and thus correlates with drip loss (Bertram et al., 2002). We explored such an interaction of thaw drip loss with spectral data obtained with BI and MW spectroscopy. To this end we added thaw drip loss (compare Fig. 2) as a co-variate to the analyses, which contrasted the three freezing treatment outcomes by using derived parameters (compare Figs. 3D and 6B for BI and MW, respectively). However, adding drip loss did not improve treatment separation, neither of MW tests based on the reflected power at 4.722 GHz, nor of BI tests based on *Py* (data not shown). This may suggest that both methods are already sensitive to water content. For MW, this is corroborated by a recent study that established a link between MW spectral data and water holding capacity of meat (Mason et al., 2016). However, with MW spectroscopy we detected a treatment effect much earlier than with thaw drip loss testing. Specifically, MW spectroscopy testing corresponds to the early '5 h' drip loss testing in Fig. 2Bi.e. was done 19 h before a treatment effect gave different drip losses ('24 h' in Fig. 2B). This suggests that MW spectroscopy is a more sensitive test for water holding capacity than EZ drip loss, or that MW is also sensitive to other quality attributes than liquid loss. For BI responses the linkage with thaw drip loss is evident by resistive elements ('availability of mobile ions') that contribute to the impedance value. However, as impedance is also a measure of capacitive elements, at least BI responses do not solely represent water content, but also describe tissue integrity, more specifically membrane integrity and cell shape (e.g., Arndt, Seebach, Psathaki, Galla, and Wegener (2004)).

3.4. The choice of statistical tools for benchmarking spectroscopic methods

Apart from comparing five analytical methods, we also provide a

Table 1
Comparison of the analytical tools.
Summary of benchmarking tests and relevant aspects for use in research and meat quality monitoring.

	Drip loss	BI	MW	NMR	Cryo-SEM
Detection capacity					
Detects fresh vs. defrosted?	O	yes	yes	yes	yes
Detects overall freeze treatment effects?	yes	yes	yes	yes	yes
Separates all 3 freeze treatments?	no	no	no	no	yes
Direct measurements in the frozen state?	no	no	no	no	yes
Implementation and users					
Equipment costs	low	moderate	moderate	very high	very high
Operating costs	cheap	cheap	cheap	high	high
Time and effort for data acquisition	fast	fast	fast	fast	slow
Expert knowledge needed for measurements?	no	no	no	yes	yes
Time and effort for analyses	low	elaborate	elaborate	elaborate	relatively low for semiquant. anal.
Expert knowledge needed for analyses?	no	yes	yes	yes	yes

statistical workflow that can be useful for future benchmark studies that can extend the range of spectroscopic methods. Direct comparability among analytical tools is necessarily limited by the nature of raw data and the specific data processing (e.g. *z* score transformations) that each method requires. At least for spectroscopic data, however, our statistical approach for analyzing raw spectral data can limit bias by parameter selection, and hence may enable better comparability among diverse spectroscopic methods.

50:50 MANOVA is an established tool for multivariate spectroscopic data (Langsrud, 2002), and allows testing of standard designs but with multiple responses. Importantly, MANOVA statistics also provide effect size estimates, with which different methods can be compared. For example, we show that low-field NMR spectra can explain a significant part of observed variance among freeze treatments (*variance explained* = 35.4%), and therefore seems to be a more reliable tool for detecting overall treatment effects than BI and MW (*variance explained* = 9.6% and 5.3%, respectively).

To identify differences between individual treatments we used a two-step approach. The first step, cross-validated PLS modeling, makes use of collinearities in spectra to compress large, multivariate data sets. In contrast to principal component analyses, PLS type regression models are efficient tools to maximize the covariance between independent variables (factors) and the spectral response (Liland, 2011). Second, the output of PLS modeling, i.e. predicted temperature values for each spectrum, could then be tested by simple ANOVA F- and post-hoc statistics (compare Figs. 3C, 4C and 6A).

In addition, PLS based statistics are useful in exploratory statistics, such as identifying relevant response characteristics for less established spectroscopic methods, e.g. for MW analyses (compare Fig. 6B and S2). However, predictions of the PLS models, in particular for MW that measured 4000 variables, need cautious examination by future studies.

We envision that the more elaborate statistical analyses discussed above are likely most relevant for benchmarking approaches. Routine measurements for quality monitoring will rather be based on testing established derived variables, such as *Py* and relaxation times for BI and NMR spectra, respectively. However, the validity of both, the analyses of raw spectra and derived parameters, is corroborated by the very similar results we obtained with the two approaches (compare Fig. 3C vs. 3D, 4C vs. 4D and 6A vs. 6B).

3.5. Methodological considerations: sample dimensions and freeze treatment detection

Effective freezing and thawing rate depends on sample dimensions, which were chosen according to the specific requirements of each analytic approach. The sample dimensions given in Section 2.1 translate into considerable volume and weight differences among samples with approximately 120 g for BI and cryo-SEM, 8.4 g for MW and 2.3 g for NMR samples. As bigger samples freeze more slowly, in particular towards the center of a sample, the benefit of lowered ambient temperatures are less manifested in larger samples. This means that the detection capacities we identified for cryo-SEM and BI – i.e. with the largest samples – are likely underestimated, when directly comparing to results obtained with MW and NMR spectroscopy. This is probably also why the bias in absolute freezing temperature prediction had the order: BI > MW = NMR.

3.6. Conclusions and technical application

Innovation in meat freezing technology is a key driver for establishing tools that can validate potential quality benefits. By testing a battery of methods our benchmarking study suggests that analytic tools should be chosen according to the particular scope of a quality assessment. Specifically, the detection capacity of the biophysical analyses as well as cryo-SEM was sufficient to distinguish fresh from defrosted meat in a direct comparison. In tests that contrasted cryogenic freezing (*CR-196C*) with two different traditional freezing solutions (*TR-25C*, *TR-35C*), all analytic tools – including thaw drip loss (larger samples and later times) – detected an overall effect of freeze treatment. Larger changes between cryogenic and traditional freezing are reflected by BI, NMR and MW spectroscopy. To also validate smaller quality improvements, e.g. among traditional freezing solutions, our data suggests quantification of cryo-SEM image data as the method of choice.

Table 1 provides a brief, simplified overview of our findings, and also lists expected advantages and downsides for the wider implementation of each analytical tool in research and industrial quality monitoring. Barriers include equipment availability and operating costs that are highest for NMR and cryo-SEM, and lowest for drip loss testing. Some tools do not require expert knowledge for operating the measuring equipment, e.g. BI and MW. For these methods, thus, future automation of the analysis workflows could open up for a wider use of BI and MW in production plants. On the other hand, the direct relevance for freeze damage is best established for thaw loss and microscopic imaging data, while the linkage between spectroscopic data and specific meat quality attributes (thaw-loss, protein denaturation etc) may be less or not yet understood (for more information on applicability see Table 1).

We consider our study an important step towards more comprehensive screenings that establish quality-monitoring tools relevant for freezing technology innovation. Yet, we want to stress that detection capacities we report here, are not universally applicable. Apart from continuous evolution of measuring instruments and analytical tools, simple adjustments to experimental designs may improve analytic performance. For example, increasing sample numbers can be a simple

and cost efficient way to improve the performance of less laborious methods, e.g., thaw loss or BI.

Acknowledgements

The Boards of the Foundation for Research Levy on Agricultural Products (FFL) and the Agricultural Agreement Research Fund (JA) are funding the project NFR 244441 Smartfrys - Almost “fresh” meat quality with novel freezing technology. The funding is channelled through the Research Council of Norway. Nortura SA, Toma Mat AS, Permanor AS and Sci Group AS are also thanked for their contribution. The Norwegian Quota Scholarship Scheme funded Sanja Krnetić and we appreciate her efforts. We also thank Ole Alvseike, Eddy Walther Hansen and Ivar Wergeland for their valuable input throughout the study. The authors declare no conflict of interest.

Appendix A. Supplementary data

Supplementary data to this article can be found online at https://doi.org/10.1016/j.meatsci.2019.02.002.

References

Agnelli, M. E., & Mascheroni, R. H. (2002). Quality evaluation of foodstuffs frozen in a cryomechanical freezer. *Journal of Food Engineering, 52*(3), 257–263 (doi: Pii S0260-8774(01)00113-3).

Arndt, S., Seebach, J., Psathaki, K., Galla, H. J., & Wegener, J. (2004). Bioelectrical impedance assay to monitor changes in cell shape during apoptosis. *Biosensors & Bioelectronics, 19*(6), 583–594.

Ballin, N. Z., & Lametsch, R. (2008). Analytical methods for authentication of fresh vs. thawed meat – A review. *Meat Science, 80*(2), 151–158. https://doi.org/10.1016/j.meatsci.2007.12.024.

Barbin, D. F., Sun, D. W., & Su, C. (2013). NIR hyperspectral imaging as non-destructive evaluation tool for the recognition of fresh and frozen-thawed porcine longissimus dorsi muscles. *Innovative Food Science and Emerging Technologies, 18*, 226–236. https://doi.org/10.1016/j.ifset.2012.12.011.

Bertram, H. C., & Andersen, H. J. (2004). Applications of NMR in meat science. In G. A. Webb (Vol. Ed.), *Annual reports on nmr spectroscopy. Vol. 53. Annual reports on nmr spectroscopy* (pp. 157–202).

Bertram, H. C., Purslow, P. P., & Andersen, H. J. (2002). Relationship between meat structure, water mobility, and distribution: A low-field nuclear magnetic resonance study. *Journal of Agricultural and Food Chemistry, 50*(4), 824–829.

Bevilacqua, A., Zaritzky, N. E., & Calvelo, A. (1979). Histological measurements of ice in frozen meat. *Journal of Food Technology, 14*(3), 237–251.

Bjarnadottir, S. G., Lunde, K., Alvseike, O., Mason, A., & Al-Shamma'a, A. I. (2015). Assessing quality parameters in dry-cured ham using microwave spectroscopy. *Meat Science, 108*, 109–114. https://doi.org/10.1016/j.meatsci.2015.06.004.

Carroll, R. J., Cavanough, J. R., & Rorer, F. P. (1981). Effects of frozen storage on the ultrastructure of Bovine Muscle. *Journal of Food Science, 46*(1091–1094), https://doi.org/10.1111/j.1365-2621.1981.tb02998.x.

Chen, T. H., Zhu, Y. P., Han, M. Y., Wang, P., Wei, R., Xu, X. L., & Zhou, G. H. (2017). Classification of chicken muscle with different freeze-thaw cycles using impedance and physicochemical properties. *Journal of Food Engineering, 196*, 94–100. https://doi.org/10.1016/j.jfoodeng.2016.10.003.

Damez, J. L., Clerjon, S., Abouelkaram, S., & Lepetit, J. (2007). Dielectric behavior of beef meat in the 1-1500kHz range: Simulation with the Fricke/Cole-Cole model. *Meat Science, 77*(4), 512–519. https://doi.org/10.1016/j.meatsci.2007.04.028.

EEC (1989). *Council directive 89/108/EEC of 21 December 1988 on the approximation of the laws of the member states relating to quick-frozen foodstuffs for human consumption.* The Council of the European Communities.

EEC (2006). *Council directive 2006/107/EC.* The Council of the European Communities.

Gottesmann, P., & Hamm, R. (1987). Grundlagen einer enzymatischen methode zur Unterscheidung zwischen Frischfleich und aufgetautem Gefrierfleisch. *Zeitschrift für Lebensmittel-Untersuchung und -Forschung, 184*, 115–121.

Hansen, E. W., & Zhu, H. (2016). Discrete and continuous spin-spin relaxation rate distributions derived from CPMG NMR response curves: A comparative analysis exemplified by water in meat. *Applied Magnetic Resonance, 47*(11), 1255–1272. https://doi.org/10.1007/s00723-016-0828-y.

Hiebel, M. (2008). *Wave quantities and S-parameters.* Rohde & Schwarz GmbH & Co.

James, C., Purnell, G., & James, S. J. (2015). A review of novel and innovative food freezing technologies. *Food and Bioprocess Technology, 8*(8), 1616–1634. https://doi.org/10.1007/s11947-015-1542-8.

Langsrud, O. (2002). 50-50 multivariate analysis of variance for collinear responses. *Journal of the Royal Statistical Society Series D-the Statistician, 51*, 305–317. https://doi.org/10.1111/1467-9884.00320.

Leygonie, C., Britz, T. J., & Hoffman, L. C. (2012). Impact of freezing and thawing on the quality of meat: Review. *Meat Science, 91*(2), 93–98. https://doi.org/10.1016/j.meatsci.2012.01.013.

Liland, K. H. (2011). Multivariate methods in metabolomics - from pre-processing to dimension reduction and statistical analysis. *Trac-Trends in Analytical Chemistry, 30*(6), 827–841. https://doi.org/10.1016/j.trac.2011.02.007.

Liu, Y., Barton, F. E., 2nd, Lyon, B. G., Windham, W. R., & Lyon, C. E. (2004). Two-dimensional correlation analysis of visible/near-infrared spectral intensity variations of chicken breasts with various chilled and frozen storages. *Journal of Agricultural and Food Chemistry, 52*(3), 505–510. https://doi.org/10.1021/jf0303464.

Martens, H., & Geladi, P. (2004). Multivariate calibration. In S. Kotz, B. Campbell, N. Balakrishnan, & B. Vidakovic (Eds.). *Encyclopedia of Statistical Science.* Wiley.

Martino, M. N., & Zaritzky, N. E. (1988). Ice crystal size modifications during frozen beef storage. *Journal of Food Science, 53*(6), 1631. (&) https://doi.org/10.1111/j.1365-2621.1988.tb07802.x.

Martinsen, O. G., Grimnes, S., & Mirtaheri, P. (2000). Non-invasive measurements of post-mortem changes in dielectric properties of haddock muscle – A pilot study. *Journal of Food Engineering, 43*(3), 189–192. https://doi.org/10.1016/S0260-8774(99)00151-X.

Mason, A., Abdullah, B., Muradov, M., Korostynska, O., Al-Shamma'a, A., Bjarnadottir, S. G., & Alvseike, O. (2016). Theoretical basis and application for measuring pork loin drip loss using microwave spectroscopy. *Sensors (Basel), 16*(2), 182. https://doi.org/10.3390/s16020182.

McDowall, A. W., Hofmann, W., Lepault, J., Adrian, M., & Dubochet, J. (1984). Cryo-electron microscopy of vitrified insect flight muscle. *Journal of Molecular Biology, 178*(1), 105–111.

Meiboom, S., & Gill, D. (1958). Modified Spin-Echo method for measuring nuclear relaxation times. *The Review of Scientific Instruments, 29*(8), 688–691. https://doi.org/10.1063/1.1716296.

Mortensen, M., Andersen, H. J., Engelsen, S. B., & Bertram, H. C. (2006). Effect of freezing temperature, thawing and cooking rate on water distribution in two pork qualities. *Meat Science, 72*(1), 34–42. https://doi.org/10.1016/j.meatsci.2005.05.027.

Ngapo, T. M., Babare, I. H., Reynolds, J., & Mawson, R. F. (1999). Freezing rate and frozen storage effects on the ultrastructure of samples of pork. *Meat Science, 53*(3), 159–168. https://doi.org/10.1016/s0309-1740(99)00051-0.

Otero, L., Rodriguez, A. C., Perez-Mateos, M., & Sanz, P. D. (2016). Effects of magnetic fields on freezing: Application to biological products. *Comprehensive Reviews in Food Science and Food Safety, 15*(3), 646–667. https://doi.org/10.1111/1541-4337.12202.

Otero, L., & Sanz, P. D. (2012). High-pressure shift freezing. In D. W. Sun (Ed.). *Handbook of frozen food processing and packaging* (pp. 667–683). Taylor & Francis Group.

Otto, G., Roehe, R., Looft, H., Thoelking, L., & Kalm, E. (2004). Comparison of different methods for determination of drip loss and their relationships to meat quality and carcass characteristics in pigs. *Meat Science, 68*(3), 401–409. https://doi.org/10.1016/j.meatsci.2004.04.007.

Park, J. H., Hyun, C. K., Jeong, S. K., Yi, M. A., Ji, S. T., & Shin, H. K. (2000). Use of the single cell gel electrophoresis assay (Comet assay) as a technique for monitoring low-temperature treated and irradiated muscle tissues. *International Journal of Food Science and Technology, 35*(6), 555–561. https://doi.org/10.1046/J.1365-2621.2000.00418.X.

Petrovic, L., Grujic, R., & Petrovic, M. (1993). Definition of optimal freezing rate. 2. Investigation of the physicalchemical properties of beef M-Longissimus Dorsi fraozen at different freezing rates. *Meat Science, 33*(3), 319–331. https://doi.org/10.1016/0309-1740(93)90004-2.

Pitera, J. W., Falta, M., & van Gunsteren, W. F. (2001). Dielectric properties of proteins from simulation: The effects of solvent, ligands, pH, and temperature. *Biophysical Journal, 80*(6), 2546–2555. https://doi.org/10.1016/s0006-3495(01)76226-1.

Plank, R. (1941). *Beiträge zur Berechnung und Bewertung der Gefriergeschwindigkeit von Lebensmitteln.* Zeitschrift f˙ur die gesamte Kälte-Industriehttps://www.tib.eu/de/suchen/id/TIBKAT%3A248941275/Beitr%C3%A4ge-zur-Berechnung-und-Bewertung-der-Gefriergeschwindigkeit/.

Pliquett, U. (2010). Bioimpedance: A review for food processing. *Food Engineering Reviews, 2*(2), 74–94. https://doi.org/10.1007/s12393-010-9019-z.

Pliquett, U., Altmann, M., Pliquett, F., & Schoberlein, L. (2003). P-y – a parameter for meat quality. *Meat Science, 65*(4), 1429–1437. https://doi.org/10.1016/s0309-1740(03)00066-4.

Prediktor (2016). *50: 50 MANOVA.* (Retrieved 10.09, 2017).

Rasmussen, A., & Andersson, M. (1996). New method for determination of drip loss in pork muscles. *Paper presented at Meat for the Consumer, Lillehammer, Norway*.

Rinnan, A., van den Berg, F., & Engelsen, S. B. (2009). Review of the most common pre-processing techniques for near-infrared spectra. *Trac-Trends in Analytical Chemistry, 28*(10), 1201–1222. https://doi.org/10.1016/j.trac.2009.07.007.

Salvadori, V. O., & Mascheroni, R. H. (2002). Analysis of impingement freezers performance. *Journal of Food Engineering, 54*(2), 133–140 (doi: Pii S0260-8774(01)00198).

Syamaladevi, R. M., Manailoh, K. N., Muhunthan, B., & Sablani, S. S. (2012). Understanding the influence of state/phase transitions on ice recrystallization in atlantic salmon (salmo salar) during frozen storage. *Food Biophysics, 7*(1), 57–71. https://doi.org/10.1007/s11483-011-9243-y.

Thyholt, K., & Isaksson, T. (1997). Differentiation of frozen and unfrozen beef using near-infrared spectroscopy. *Journal of the Science of Food and Agriculture, 73*(4), 525–532.

Townes, C. H., & Schawlow, A. L. (2012). *Microwave spectroscopy.* Mineolo, NewYork: Dover Publication Inc.

Vanhonacker, F., Pieniak, Z., & Verbeke, W. (2013). European consumer perceptions and barriers for fresh, frozen, preserved and ready-meal fish products. *British Food Journal, 115*(4), 508–525. https://doi.org/10.1108/00070701311317810.

Ward, L. C., Hopkins, D. L., Dunshea, F. R., & Ponnampalam, E. (2016). Evaluating meat quality with bioelectrical impedance spectroscopy. Paper presented at the 8th annual scientific meeting of the Nutrition Society of Australia. At Hobart, Volume *Journal of Nutrition and Intermediary Metabolism, 1*, 52.

Warriss, P. (2010). Meat hygiene, spoilage and preservation meat science (pp. 142). Oxfordshire, UK: CABI.

Wolschin, F., Münch, D., & Amdam, G. V. (2009). Structural and proteomic analyses reveal regional brain differences during honeybee aging. *The Journal of Experimental Biology, 212*(Pt 24), 4027–4032. https://doi.org/10.1242/jeb.033845.

Zhao, X., Zhuang, H., Yoon, S. C., Dong, Y. G., Wang, W., & Zhao, W. (2017). Electrical impedance spectroscopy for quality assessment of meat and fish: A review on basic principles measurement methods, and recent advances. *Journal of Food Quality, 6370739*. https://doi.org/10.1155/2017/6370739 Artn.